

## Tunable photonic strength in porous GaP

J. Gómez Rivas<sup>a)</sup> and A. Lagendijk<sup>a),b)</sup>

*Van der Waals-Zeeman Instituut, Universiteit van Amsterdam, Valckenierstraat 65,  
1018 XE Amsterdam, The Netherlands*

R. W. Tjerkstra,<sup>c)</sup> D. Vanmaekelbergh, and J. J. Kelly

*Debye Instituut, Universiteit Utrecht, Post Office Box 80000, 3508 TA Utrecht, The Netherlands*

(Received 21 September 2001; accepted for publication 22 April 2002)

The light-scattering properties of porous gallium phosphide, prepared by electrochemical etching, are investigated. We show that the photonic strength of the porous semiconductor can be tuned from weak to extremely strong. This tunability is related to the density and size of the pores, which are controlled by the dopant density of the GaP crystals, and the etching potential. Moreover, electrochemical etching does not introduce any significant optical absorption, which makes porous GaP suitable for many photonic applications. © 2002 American Institute of Physics.

[DOI: 10.1063/1.1485316]

Photonic materials interact strongly with light as a result of a variation of the refractive index  $n$  on length scales of the order of the optical wavelength  $\lambda$ . The field of photonic materials has undergone a spectacular growth<sup>1</sup> due to the wide range of applications that they have: efficient light-emitting diodes, low-threshold lasers, microcavities, waveguides, and fast optical switches. In addition, photonic systems exhibit fascinating fundamental phenomena, such as inhibition of spontaneous emission and light localization.

Pore formation by means of electrochemical etching has emerged as a very promising technique for tailoring the photonic properties of semiconductors. Most electrochemical studies have focused on silicon (Si) (Ref. 2) rather than on GaP. Si is transparent only for infrared radiation  $\lambda > 1.1 \mu\text{m}$ . In contrast, gallium phosphide (GaP) is transparent for light in the yellow and red part of the visible spectrum  $\lambda > 0.55 \mu\text{m}$ . This absence of optical absorption, together with its very high refractive index ( $n = 3.3$ ),<sup>3</sup> makes GaP a fascinating material for optical applications in the important wavelength range,  $0.55 \mu\text{m} < \lambda < 1.1 \mu\text{m}$ , a range where Si shows strong absorption. In spite of this advantage, up until now, relatively little work has been performed on porous GaP.<sup>4</sup> Only recently, a first study of the photonic strength of porous GaP was reported:<sup>5</sup> strong scattering of visible light without optical absorption was measured.

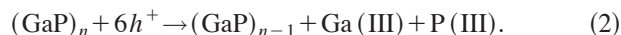
In this letter, we show that it is easy to tune the photonic strength of porous GaP in a wide range by controlling the density and size of the pores. This tailoring can be achieved by using  $n$ -type GaP crystals with different dopant densities and by varying the etching potential. Moreover, since no optical absorption could be detected in any of the samples, porous GaP is suitable for photonic applications in the visible spectrum: these include diffuse reflectors, Bragg reflectors, and random lasers.

The photonic strength is defined in terms of the transport mean free path  $\ell$ , which is the average length required to randomize the direction of propagation of the light by scattering. A small value of  $\ell$  corresponds to efficient scattering or high photonic strength. The transport mean-free path is given by

$$\ell = \frac{1}{\rho\sigma}, \quad (1)$$

where  $\rho$  is the density of scatterers and  $\sigma$  is the transport cross section.<sup>6</sup> In our samples the pores are the scatterers, so the density of scatterers is determined by the pore density. For a given refractive-index contrast,  $\sigma$  depends to a large extent on the size of the scatterers relative to the wavelength of light.<sup>7</sup> The largest cross section is achieved when the size of the scatterers, or in our case the pore diameter, is close to the optical wavelength, i.e., in the Mie-scattering regime.<sup>7</sup>

An  $n$ -type GaP electrode does not dissolve anodically in the dark at potentials below  $\sim 5$  V. Valence band holes are required for the dissolution reaction



However, when the anode potential is strongly positive, electrons can tunnel from the valence to the conduction band, a process known as breakdown. The holes generated in this way cause etching according to reaction (2), and give rise to a porous structure.<sup>8</sup> Etching does not proceed preferentially along crystallographic orientations, and a highly isotropic porous structure is formed. From the autocorrelate of scanning-electron-microscope (SEM) images, it can be concluded that the porous structure is statistically homogeneous and that it does not present short-range order.<sup>5</sup> Above a potential denoted as  $V_{\text{max}}$ , the electrode becomes passivated due to the formation of an oxide layer.<sup>9</sup>  $V_{\text{max}}$  constitutes the upper limit for the etching potential.

In our experiments, the starting materials were commercially available  $n$ -type GaP wafers, (100) oriented, doped

<sup>a)</sup>Present address: Faculty of Applied Physics, University of Twente, Post Office Box 217, 7500 AE Enschede, The Netherlands.

<sup>b)</sup>Author to whom correspondence should be addressed; electronic mail: a.lagendijk@tn.utwente.nl

<sup>c)</sup>Present address: MESA+ Research Institute, University of Twente, Post Office Box 217, 7500 AE Enschede, The Netherlands.

TABLE I. Porosity  $\phi$ , average pore diameter  $d$ , interpore distance  $X$ , and transport mean-free path  $\ell$  of porous GaP of dopant density  $N$ , etched at a potential  $V$ .  $V_{\max}$  is the maximum potential at which electrochemical etching is possible.

$N$ ( $10^{17} \text{ cm}^{-3}$ )	$V$ (V)	$\phi$ (%)	$d$ ( $\mu\text{m}$ )	$X$ ( $\mu\text{m}$ )	$\ell$ ( $\mu\text{m}$ )
4–6	$16.6 = V_{\max}$	67	$0.19 \pm 0.04$	$0.15 \pm 0.03$	$0.22 \pm 0.02$
6	$12.7 = V_{\max}$	62	$0.12 \pm 0.03$	$0.10 \pm 0.03$	$0.46 \pm 0.04$
7	$11.2 = V_{\max}$	62	$0.09 \pm 0.03$	$0.08 \pm 0.03$	$0.8 \pm 0.03$
10–20	$7.8 = V_{\max}$	93	$< 0.06$	$< 0.06$	$1.1 \pm 0.1$
4–6	15	40	$0.10 \pm 0.03$	$0.15 \pm 0.04$	$0.43 \pm 0.03$
10–20	7.4	65	$< 0.06$	$< 0.06$	$1.24 \pm 0.1$

with sulfur to different donor densities,  $N=4-6,6,7$  and  $10-20 \times 10^{17} \text{ cm}^{-3}$ .<sup>10</sup> The electrochemical etching was done in an aqueous 0.5 M  $\text{H}_2\text{SO}_4$  solution.<sup>9</sup>

From Table I, we observe that  $V_{\max}$  increases as the dopant density decreases. As for anodically etched Si,<sup>11</sup> the pore diameter, interpore distance, and porosity of GaP depend on the dopant density and on the applied potential. The porosity can be calculated from the charge passed during etching and the porous-layer thickness. The pore diameter and interpore distance can be estimated from high-magnification SEM images. In Table I, we list the porosity  $\phi$ , pore diameter  $d$ , and interpore distance  $X$  of samples with different dopant density etched at  $V_{\max}$ . We also present results for GaP etched at  $V < V_{\max}$ . As can be concluded from the Table I, anodic etching at  $V < V_{\max}$  produces a structure with smaller pores and lower porosity. Therefore, the pore diameter and the pore density can be controlled in a wide range by tuning the applied potential.

To characterize the photonic strength of the samples, we have obtained the transport mean-free path from enhanced backscattering (EBS) measurements. EBS refers to an increase of the reflected intensity from a disordered multiple-scattering sample at exactly the backscattering direction.<sup>12</sup> This increase is due to interference of waves propagating along time-reversed optical paths. The EBS yields a cone in the plot of the backscattered intensity versus the scattering angle. The full width at half maximum  $W$  of the EBS cone is directly related to the transport mean free path  $\ell$ . For a non-absorbing and semi-infinite sample, this relation is  $\ell \approx 0.7\lambda(1-\bar{R})/2\pi W$ ,<sup>13</sup> where  $\bar{R}$  is the angular and polarization-averaged internal reflection at the sample boundary.<sup>14</sup>

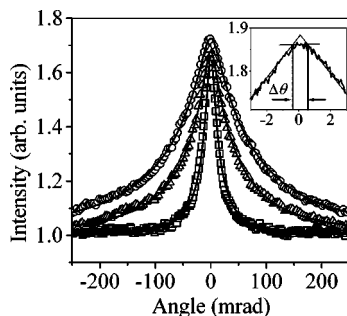


FIG. 1. Enhanced backscattering measurements of porous GaP with different dopant densities  $N=10-20$  ( $\square$ ),  $6$  ( $\diamond$ ),  $4-6$  ( $\circ$ )  $\times 10^{17} \text{ cm}^{-3}$ . All samples have a porosity of  $\approx 65\%$ . The solid lines on top of the measurements are fits using diffusion theory. Inset: Detailed measurement of the top of the EBS cone of a sample with a thickness  $L=203 \mu\text{m}$ .  $\Delta\theta$  represents the rounding of the cone due to the finite thickness.

The EBS measurements were performed using the off-centered rotation technique<sup>15</sup> with a He:Ne laser as light source ( $\lambda=633 \text{ nm}$ ). The optical absorption in porous GaP was investigated with detailed measurements of the top of the EBS cones. Optical absorption and the finite thickness of the samples cause a rounding of the cone.<sup>16</sup> Our thickest sample has a thickness of  $L=203 \mu\text{m}$ . The corresponding cone rounding for such a sample thickness in the absence of absorption is predicted to be  $\Delta\theta=1.0 \text{ mrad}$ . The top of the cone of this sample is plotted in the inset of Fig. 1. The rounding is  $\Delta\theta=0.9 \pm 0.2 \text{ mrad}$ , in good agreement with the value expected for a nonabsorbing sample given our experimental accuracy. We conclude that at  $\lambda=633 \text{ nm}$ , the absorption length of porous GaP  $L_a \geq 200 \mu\text{m}$ , which means that there is virtually no optical absorption in electrochemically etched GaP.

The EBS results of porous GaP samples with different dopant densities are plotted in Fig. 1. The samples were prepared with the same porosity  $\phi \approx 65\%$ . For the  $N=4-6,6,7 \times 10^{17} \text{ cm}^{-3}$  samples, the etching potential was  $V_{\max}$ . The sample with  $N=10-20 \times 10^{17} \text{ cm}^{-3}$  was etched at  $7.4$ , i.e.,  $V < V_{\max}$ . Although the porosity of these samples is similar, the average pore size and interpore distance are bigger for lower  $N$  (see Table I and inset of Fig. 2). As is clear from Fig. 1, the EBS cone is wider for lower  $N$ , indicating stronger scattering or shorter  $\ell$ .

To obtain  $\ell$  from the EBS measurements, the internal reflection at the boundary  $\bar{R}$  needs to be known.  $\bar{R}$  can be calculated from the effective refractive index  $n_e$  of the sample.<sup>14</sup> From angular-resolved transmission measurements,<sup>17</sup> we find  $n_e$  in the range  $1.35-1.55$  for all the samples with a porosity of  $65\%$ . With  $n_e=1.45$ , an internal reflection coefficient  $\bar{R}$  of  $0.5$  is calculated. The transport mean-free paths are obtained from the fits of diffusion

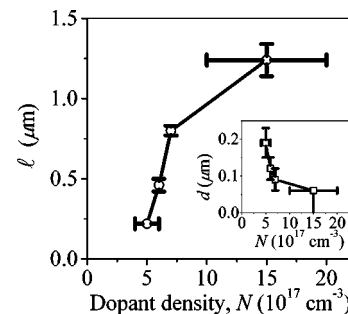


FIG. 2. Transport mean free path  $\ell$  of porous GaP samples with a porosity of  $\approx 65\%$  as function of the dopant density. Inset: average pore size of the same samples. The solid lines are guides for the eye.

theory<sup>13</sup> to the EBS measurements, shown as solid lines in Fig. 1, taking  $\bar{R}=0.5$  and considering the finite thickness of the samples. In Fig. 2,  $\ell$  is plotted versus the dopant density. A quantitative description of this dependence of  $\ell$  with  $N$  is difficult. Theories for strongly scattering media are only valid in systems formed by spherical or cylindrical scatterers.<sup>18</sup> The irregular shape of the pores and the complicated porous structure hampers this description. However, a qualitative description based on Eq. (1) is possible. The decrease of the transport mean-free path, by more than a factor of 5 for the lowest doped GaP with respect to the highest doped sample, is due to the increase of the pore diameter: the bigger the pore diameter becomes, the larger is the transport cross section.<sup>7</sup> For the sample with  $N=4-6 \times 10^{17} \text{ cm}^{-3}$ , we find  $\ell=0.22 \pm 0.02 \mu\text{m}$ . This is the strongest scattering medium of visible light found to date.

The relatively short transport mean-free path of the highly doped GaP sample ( $\ell=1.24 \pm 0.07 \mu\text{m}$ ) can be understood in terms of the large density of scatterers. The cross section  $\sigma$  is expected to be very low, due to the small pore size ( $d < 0.06 \mu\text{m}$ ), but the small pore separation leads to a high density  $\rho$ , which is responsible for a short mean-free path.

The optical and scattering properties of porous GaP open the way to various photonic applications. Strongly scattering porous layers are virtually perfect diffuse reflectors. A 200  $\mu\text{m}$  thick layer of low-doped GaP etched at  $V_{\text{max}}$  has a diffuse reflection larger than 99%. Moreover, the reflection can be easily regulated by controlling the photonic strength and/or the layer thickness. By introducing into the GaP porous structure an emission source, such as quantum dots or an organic dye, strongly scattering random lasers are feasible. Multilayers of low porosity GaP are easy to make.<sup>9</sup> Such multilayers could be used as efficient one-dimensional photonic crystals or Bragg reflectors. Besides photonic applications, porous GaP can be used for micromechanical devices and sieves for biomolecules in micro total analysis systems.

We have shown that anodic etching of  $n$ -type GaP produces a random porous structure that strongly scatters light, without introducing any measurable optical absorption. The photonic strength of porous GaP can be tuned in a wide range, since the pore size (cross section of the scatterers) and distance between pores (density of scatterers) depend strongly on the dopant density and on the potential applied during the etching. This capability to tune the photonic strength opens the possibility of multiple applications. The strongest-scattering samples ( $\ell=0.22 \mu\text{m}$  at  $\lambda=633 \text{ nm}$ )

are made from low-doped GaP ( $N=4-6 \times 10^{17} \text{ cm}^{-3}$ ) etched at the maximum possible potential. These samples are the strongest-scattering media of visible light.

The authors thank B. Bret, P. Johnson, T. Hijmans, F. J. P. Schuurmans, and G. van Soest for fruitful discussions, W. Takkenberg and X. Xinghua for assistance with the SEM, S. Zevenhuizen for technical backup, and W. L. Vos for reading this manuscript. They also thank Hewlett Packard and Philips for supplying us with some of the GaP wafers. This work is part of the research program of the Stichting voor Fundamenteel Onderzoek der Materie, which is supported by the Nederlandse Organisatie voor Wetenschappelijk Onderzoek. Part of the work was funded by NWO Gebied Chemische Wetenschappen.

<sup>1</sup> *Photonic Crystals and Light Localization in the 21st Century*, edited by C. M. Soukoulis (Kluwer, Dordrecht, 2001).

<sup>2</sup> A. G. Cullis, L. T. Canham, and P. D. J. Calcott, *J. Appl. Phys.* **82**, 909 (1997), and references therein.

<sup>3</sup> A. Borghesi and G. Guizzetti, in *Handbook of Optical Constants of Solids*, edited by E. D. Palik (Princeton, New York, 1952), p. 445.

<sup>4</sup> J. J. Kelly and D. Vanmaekelbergh, in *The Electrochemistry of Nanomaterials*, edited by G. Hodes (Wiley-VCH, Weinheim, 2001), Chap. 4, and references therein.

<sup>5</sup> F. J. P. Schuurmans, D. Vanmaekelbergh, J. van de Lagemaat, and A. Lagendijk, *Science* **284**, 141 (1999).

<sup>6</sup> A. Ishimaru, *Wave Propagation and Scattering in Random Media* (Academic, New York, 1978), Vol. 1, p. 178.

<sup>7</sup> H. C. van de Hulst, *Light Scattering by Small Particles* (Dover, New York, 1957).

<sup>8</sup> A. Etcheberry, J. L. Sculfort, and A. Marbeuf, *Sol. Energy Mater.* **3**, 347 (1980); B. H. Erné, D. Vanmaekelbergh, and J. J. Kelly, *J. Electrochem. Soc.* **143**, 305 (1996).

<sup>9</sup> R. W. Tjerkstra, J. Gómez Rivas, D. Vanmaekelbergh, and J. J. Kelly, *Electrochem. Solid-State Lett.* **5**, G32 (2002).

<sup>10</sup> The dopant densities were specified by the suppliers of the GaP wafers: Hewlett Packard, Philips, Atomergerie Chemetals, and Ramet Ltd.

<sup>11</sup> M. I. J. Beale, J. D. Benjamin, M. J. Urem, N. G. Chew, and A. G. Cullis, *J. Cryst. Growth* **73**, 622 (1985); P. C. Searson, J. M. Macaulay, and F. M. Ross, *J. Appl. Phys.* **72**, 253 (1992); X. G. Zhang, *J. Electrochem. Soc.* **138**, 3750 (1991).

<sup>12</sup> M. P. Albada and A. Lagendijk, *Phys. Rev. Lett.* **55**, 2692 (1985); P. E. Wolf and G. Maret, *ibid.* **55**, 2696 (1985).

<sup>13</sup> M. B. van der Mark, M. P. van Albada, and A. Lagendijk, *Phys. Rev. B* **37**, 3575 (1988).

<sup>14</sup> J. X. Zhu, D. J. Pine, and D. A. Weitz, *Phys. Rev. A* **44**, 3948 (1991).

<sup>15</sup> D. S. Wiersma, M. P. van Albada, and A. Lagendijk, *Rev. Sci. Instrum.* **66**, 5473 (1995).

<sup>16</sup> I. Edrei and M. Kaveh, *Phys. Rev. B* **35**, R6461 (1987); S. Etemad, R. Thompson, M. J. Andrejco, S. John, and F. C. MacKintosh, *Phys. Rev. Lett.* **59**, 1420 (1987).

<sup>17</sup> M. U. Vera and D. J. Durian, *Phys. Rev. E* **53**, 3215 (1996); A. Lagendijk, J. Gómez Rivas, A. Imhof, F. J. P. Schuurmans, and R. Sprik, in *Photonic Crystals and Light Localization in the 21st Century*, edited by C. M. Soukoulis (Kluwer, Dordrecht, 2001), pp. 447–473.

<sup>18</sup> K. Busch and C. M. Soukoulis, *Phys. Rev. Lett.* **75**, 3442 (1995).